

The British University in Egypt

BUE Scholar

Pharmacy

Health Sciences

Fall 9-20-2023

Design, molecular modelling and synthesis of novel benzothiazole derivatives as BCL-2 inhibitors

Amira Khalil

The British University in Egypt, amira.khalil@bue.edu.eg

Hoda S. Ismail

Ain Shams University

Dalal A. Abou El Ella

Ain Shams University, dalal@pharma.asu.edu.eg

Deena S. Lasheen

Ain Shams University, deenalasheen@pharma.asu.edu.eg

Rabah A. Taha

Ain Shams University

Follow this and additional works at: <https://buescholar.bue.edu.eg/pharmacy>



Part of the [Chemicals and Drugs Commons](#), and the [Medicinal and Pharmaceutical Chemistry Commons](#)

Recommended Citation

Khalil, Amira; Ismail, Hoda S.; Abou El Ella, Dalal A.; Lasheen, Deena S.; and Taha, Rabah A., "Design, molecular modelling and synthesis of novel benzothiazole derivatives as BCL-2 inhibitors" (2023). *Pharmacy*. 766.

<https://buescholar.bue.edu.eg/pharmacy/766>

This Article is brought to you for free and open access by the Health Sciences at BUE Scholar. It has been accepted for inclusion in Pharmacy by an authorized administrator of BUE Scholar. For more information, please contact bue.scholar@gmail.com.



OPEN

Design, molecular modelling and synthesis of novel benzothiazole derivatives as BCL-2 inhibitors

Hoda S. Ismail¹, Amira Khalil²✉, Rabah A. Taha¹, Deena S. Lasheen¹ & Dalal A. Abou El Ella¹✉

Apoptosis plays a crucial role in cancer pathogenesis and drug resistance. BCL-2 family of enzymes is considered as one of the key enzymes which is involved in apoptosis. When there is disruption in the balance between anti-apoptotic and pro-apoptotic members of the BCL-2 family apoptosis is dysregulated in the affected cells. Herein, 33 novel benzothiazole-based molecules 7a-i, 8a-f, 9a-b, 12a-e, 13a-d, 14a,b, and 17a-j were designed, synthesized and tested for their BCL-2 inhibitory activity. Scaffold hopping strategy was applied in designing of the target compounds. Compounds 13c and 13d showed the highest activity with IC₅₀ values equal to 0.471 and 0.363 μM, respectively. Molecular docking studies of the synthesized compounds showed comparable binding interactions with the lead compound. Structure activity relationship study was performed to show the effects of structural modifications on the inhibitory activities on BCL-2.

Cancer is considered a leading cause of death worldwide accounting for about 14.5% of world deaths, and it is expected for that ratio to double by 2030¹. The concept of "Hallmarks of Cancer" is a powerful guide for research aimed to improving and developing rational approaches for more targeted cancer therapeutics². The ability of cancer cells to resist cell death and evade apoptosis, which leads to continuous proliferation, is one of the fundamental hallmarks of cancer. Therefore, it has become a major area of interest in the development of targeted cancer therapy.

Apoptosis is a physiological process of programmed cell death that is essential for normal tissue development and hemostasis³. Aberrations in this pathway can lead to a variety of diseases including degenerative and autoimmune disorders and cancer^{4,5}.

Caspases is a family of enzymes that plays a critical role in apoptosis regulation⁶. Caspases are synthesized as inactive zymogens, which undergo activation through cascade of events known collectively as either intrinsic or extrinsic pathways^{7,8}.

Cancer cells may evade apoptosis through a variety of mechanisms. In human cancer cells, the downregulation of pro-apoptotic proteins (e.g. Bax, Bak, Bad, Bim) and the upregulation of anti-apoptotic proteins (e.g. BCL-2, BCL-xl, MCL-1), inhibits the release of cytochrome *c* from mitochondria, leads to the immortal character of the cancer cells⁹. In cancer cell lines, all the apoptotic inhibitors and activators have been found to be expressed abnormally. For instance, in almost half of all human cancers, BCL-2 overexpression has been found¹⁰.

BCL-2 family proteins are the key regulators of the mitochondrial apoptotic pathway, also known as the BCL-2-regulated pathway. There are 25 members that belong to the BCL-2 family of proteins. These proteins are found in mitochondria, smooth endoplasmic reticulum, and perinuclear membranes in hematopoietic cells^{11,12}. The structure of BCL-2 proteins are known to exhibit up to four relatively short sequence motifs, which are less than 20 amino acid residues in length, termed BCL-2 homology (BH) domains^{13,14}. All BCL-2 family proteins present BCL-2 homology (BH) domains, with the most conserved BH3 death domain being found in all members of the family. Members of BCL-2 family can be divided into three subfamilies based on structural and functional features¹⁵⁻¹⁷ which include anti-apoptotic multi-domain proteins, pro-apoptotic BH3-only proteins and pro-apoptotic multi-domain effector proteins. The functions of BCL-2 family members including the anti-apoptotic and pro-apoptotic are regulated through their BH domains. Furthermore, the BH1- BH3 domains of anti-apoptotic proteins form a hydrophobic binding pocket that binds the α-helix of the BH3-only pro-apoptotic

¹Pharmaceutical Chemistry Department, Faculty of Pharmacy, Ain Shams University, Cairo, Egypt. ²Pharmaceutical Chemistry Department, Faculty of Pharmacy, The British University in Egypt (BUE), El-Sherouk City, Cairo 11837, Egypt. ✉email: Amira.Khalil@bue.edu.eg; dalal@pharma.asu.edu.eg

proteins^{18,19}. If there is imbalance between the anti-apoptotic and pro-apoptotic members of the BCL-2 family, it will result in dysregulated apoptosis in the affected cells. This could be attributed to the expression of one or more anti-apoptotic proteins or the low expression of one or more pro-apoptotic proteins or a combination of both²⁰.

The selective modulation of both apoptotic pathways has been reported to be a challenge in cancer drug development. BCL-2 functions by preventing programmed cell death which differs from other oncogenes that work mainly by enhancing proliferation²¹. Therefore, inhibiting these proteins would lead to apoptosis induction which could provide potential therapeutic target²². However, the critical challenge is that many of these targets are protein–protein interactions and it is hard to modulate. Despite this, there are various promising molecules which target the apoptotic pathway components that have now entered the clinic, and are under investigation as single agents or in combination with other anticancer therapies²³. Anti-sense oligonucleotides (ASOs), peptides and peptidomimetics as well as small molecules (BH3 mimetics) are among the promising BCL-2 inhibitors. Despite the emergence of various BCL-2 inhibitors, there are many challenges that are facing these inhibitors, including the development of resistance and limitation of their use in certain types of tumors, e.g., solid tumors. These challenges encourage many researchers to search, design and synthesize novel BCL-2 inhibitors with better activity, less resistance and safer profile²⁴.

Figure 1 shows some of BCL-2 inhibitors in which the structural features and the important interactions are highlighted^{25–29}.

Rationale and design

Our proposed design of novel benzothiazole based inhibitors was according to the strategies shown in (Fig. 2). Scaffold hopping strategy has been used for designing structurally novel compounds by modifying the central core of an active molecule. Thus, the saccharine scaffold in the lead compound **2** has been replaced by benzothiazole scaffold. The introduction of heterocyclic core will lead to increased acidity of the sulfonamide NH which is proposed to influence potency, solubility, and clearance of these inhibitors. Additionally, the benzothiazole scaffold will maintain the proper orientation of the two essential hydrophobic pocket binding moieties of the compound. The sulfonamide moiety has been retained in most of proposed compounds. In other compounds, it has been replaced by its amide bioisostere to maintain crucial hydrogen bond interactions. Furthermore, a number of diverse small and large hydrophobic moieties with different substituents have been utilized, which maintain the reported hydrophobic interaction with P2 pocket, to explore the hydrophobic moiety with optimum BCL-2 inhibitory activity. Similarly, based on the reported hydrophobic groups used as the P4 binding moieties, the naphthyl (as in compound **1**) and 3-nitro-4-(phenethylamino)benzene (to mimic the P4 hydrophobic moiety in compound **2**) have been used to maintain desirable hydrophobic interaction with P4 pocket and to explore the hydrophobic moiety with optimum BCL-2 inhibitory activity. Finally, the piperazine linker between the core scaffold and the P2 hydrophobic moiety has been retained in some proposed compounds or replaced by other linkers such as urea and amide linkers in other compounds to explore their impact on BCL-2 inhibitory activity.

The aim of the current study is to rationally design, synthesize and biologically evaluate novel small molecule BCL-2 inhibitors (BH3 mimetics) via targeting the BH3 binding groove of anti-apoptotic BCL-2 protein as targeted anti-cancer therapy.

Materials and methods

Chemistry. Starting materials and reagents were purchased from Sigma-Aldrich or Alfa-Aesar Organics and used without further purification. Reactions were monitored by analytical TLC, performed on silica gel 60 F₂₅₄ packed on Aluminum sheets, purchased from Merck, with visualization under UV light (254 nm). Melting points were recorded on Stuart Scientific apparatus and are uncorrected. Electron-impact ionization mass (EI-MS) spectra were recorded on Thermo Scientific ISQLT mass spectrometer at the Regional Center for Mycology and Biotechnology, Al-Azhar University.

¹H-NMR spectra were recorded using Bruker 400 MHz spectrophotometer (using DMSO as solvent) at Center for Drug Discovery Research and Development, Ain Shams University. ¹³C-NMR spectra were recorded in δ scale given in ppm on a Bruker 100 MHz spectrophotometer (at 101 MHz, using DMSO as solvent) at Center for Drug Discovery Research and Development, Ain Shams University. Elemental analyses were performed on a Thermo Scientific Flash 2000 elemental analyzer at the Regional Center for Mycology and Biotechnology, Al-Azhar University.

For the detailed synthetic procedures and structural characterization, refer to the supporting information.

Biological evaluation. *In vitro BCL-2 inhibitory activity.* The *in vitro* enzyme inhibition determination for the synthesized compounds was carried out in BPS Bioscience Corporation, San Diego, CA, USA (www.bpsbioscience.com). BCL-2: Catalog # 50272, BCL-2 binding peptide, BCL-2 Assay Kit: Catalog #50222, and Tb-Donor and Dye labeled acceptor were used.

Assay protocol. The assay was performed by TR-FRET technology using a recombinant BCL-2 and a peptide-ligand substrate. The TR-FRET signal from the assay is correlated with the amount of Ligand binding to BCL-2. Compounds were diluted in 100% DMSO then tenfold dilution in 10% DMSO in 1X Reaction Buffer. 2 μ l of the dilution was added to a 20 μ l reaction so that the final concentration of DMSO is 1% in all of reactions. All of the binding reactions were conducted at room temperature. The 20 μ l reaction mixture in Assay Buffer contains bcl-2, the indicated amount of the inhibitor, ligand, and the reaction dyes. The reaction mixture incubated for 180 min prior to reading the TR-FRET signal. For the background, ligand was replaced with assay buffer. Fluorescence signals for both the donor and acceptor dyes were measured using a Tecan Infinite M1000 plate reader. TR-FRET was recorded as the ratio of the fluorescence of the acceptor and the donor dyes (acceptor/donor).

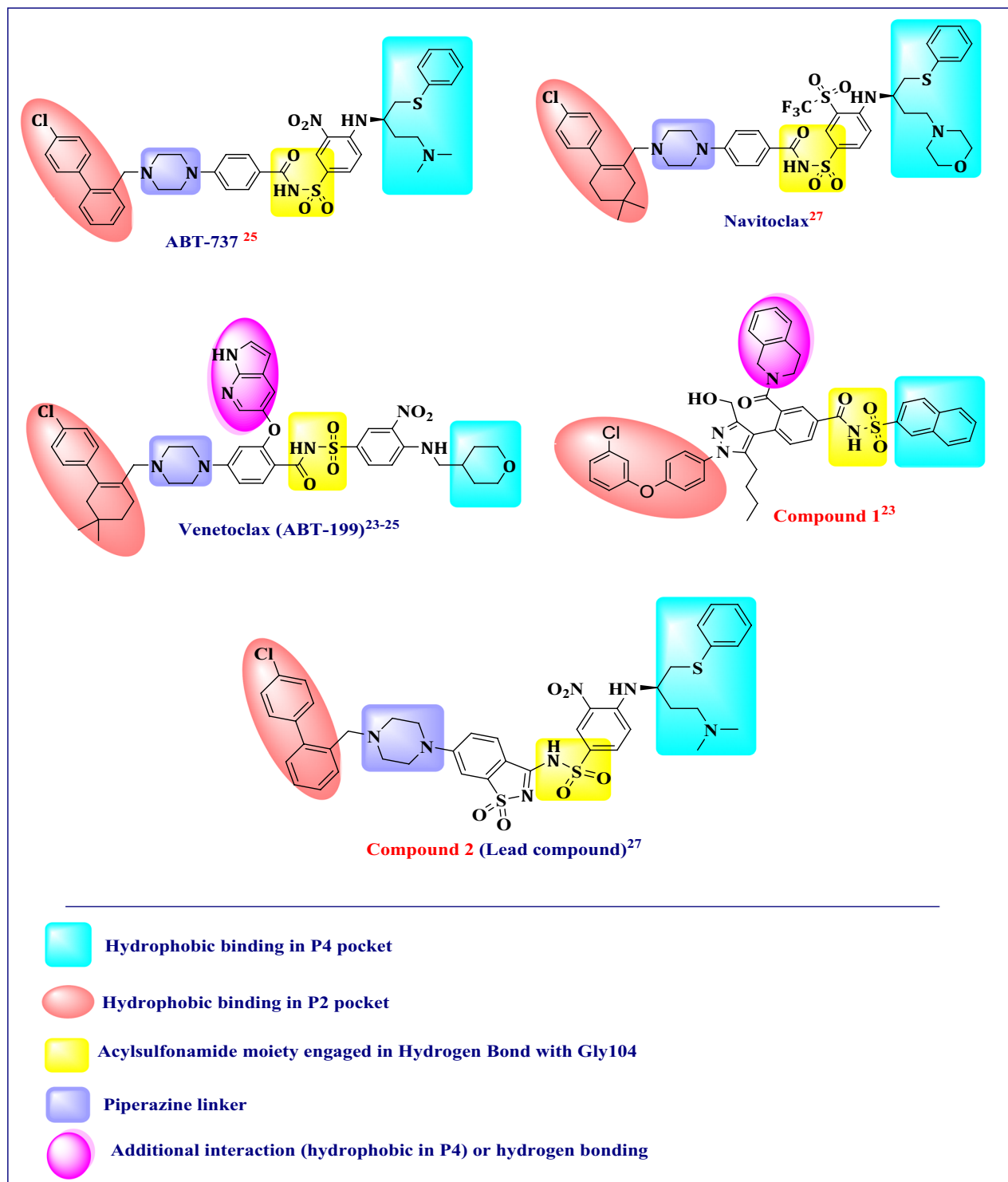


Figure 1. The common structural features and the possible key interactions of prominent BCL-2 inhibitors with BCL-2 protein. Figure 1 was generated using Chemdraw Professional 16.0.

Binding experiments were performed in duplicate at each concentration. The TR-FRET data were analyzed using the computer software, Graphpad Prism. In the absence of the compound in wells containing BCL-2 ligand, the TR-FRET signal (Ft) in each data set was defined as 100% activity. In wells without peptide ligand, the TR-FRET signal (Fb) in each data set was defined as 0% activity. The percent activity in the presence of each compound was calculated according to the following equation: % activity = $[(F - F_b) / (F_t - F_b)] \times 100$, where F = the TR-FRET signal in the presence of the compound. The percent inhibition was calculated according to the following equation: % inhibition = $100 - \% \text{ activity}$. IC₅₀ determination for target

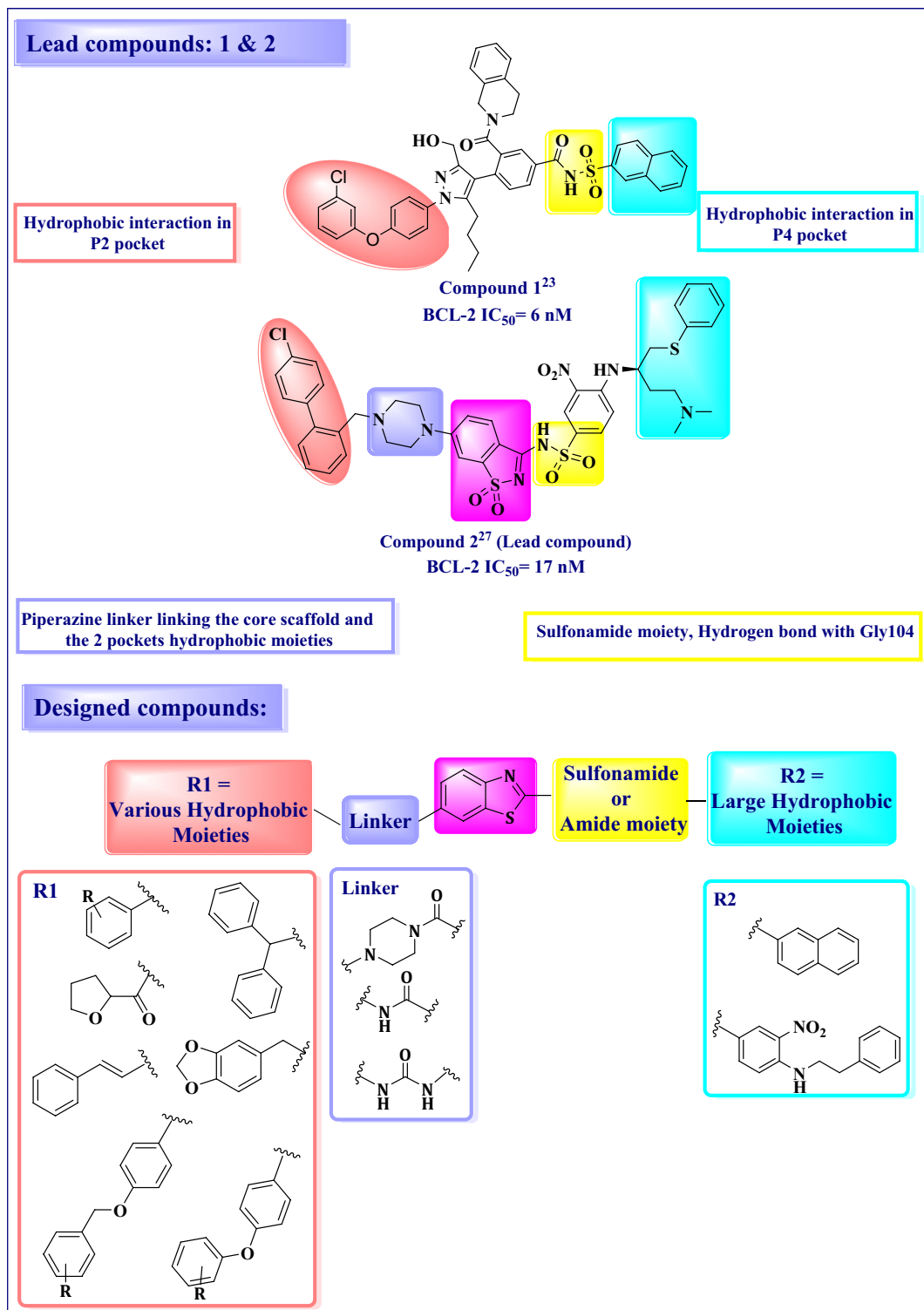


Figure 2. Proposed design of novel benzothiazole based small molecule BCL-2 inhibitors. Figure 2 was generated using Chemdraw Professional 16.0.

compounds against BCL-2 was calculated. The values of % activity versus a series of compound concentrations (1 nM–10 nM–100 nM–1 μM–10 μM) were then plotted using non-linear regression analysis of Sigmoidal dose–response curve generated with the equation:

$$Y = B + (T - B) / (1 + 10^{((\text{LogEC}_{50} - X) \times \text{Hill Slope})})$$

where, Y = percent activity, B = minimum percent activity, T = maximum percent activity, X = logarithm of compound and Hill Slope = slope factor or Hill coefficient. The IC₅₀ value was determined by the concentration causing a half-maximal percent activity³⁰.

In vitro anti-proliferative activity against NCI leukemia cell line. The national cancer institute (NCI) in vitro anticancer screening is a two-stage process, beginning with the evaluation of the selected compounds **13c** and **13d** against NCI leukemia cell line at a single dose of 10 μM. The human leukemia cell line was obtained and maintained at the NCI. The output from the single dose screen is reported as a mean graph. The detailed assay protocol is discussed in the supporting material.

Molecular modelling study. Molecular docking was conducted using C-Docker 2.5 software in the interface of Accelry's discovery studio 2.5 (Accelrys Inc., San Diego, CA, USA) at the drug design laboratory of Faculty of pharmacy, Ain Shams university. The X-ray crystal structure of BCL-2 co-crystallized with saccharine-based lead compound **2** was obtained from the Protein Data Bank³¹ with PDB code: **4IEH**²⁹. This PDB code was chosen to compare the docked poses of our designed compounds to the lead compound **2**. Protein was prepared in Discovery Studio 2.5 by deleting water molecules and adding hydrogen atoms. A final step of energy minimization for hydrogen atoms was done to relieve the constraints resulting from randomly adding hydrogen atoms with constraining protein heavy atoms. Docking search space was identified by assigning a sphere centred around the co-crystallized ligand including the surrounding amino acids of the binding site. The docking sphere had a centre at coordinates 12.2, 25.8, 11.8, and a radius of 60 Å.

Ligands were sketched in ChemDraw and minimized in Discovery Studio 2.5 using CHARMM force field adjusting the ionization pH at 7.4, with no isomers or tautomers generated for the ligands. Figures were generated using UCSF Chimera³² and Discovery Studio 2.5. Physicochemical and drug likeness properties are predicted using SwissADME webserver (<https://www.nature.com/articles/srep42717>).

Results and discussion

Chemistry. The titled compound (**5**) was prepared in good yield and purity via nucleophilic substitution of the 2-aminobenzothiazole derivatives (**4**) on 2-naphthylsulfonyl chloride in dry pyridine.

Compound (**6**) was obtained through ester hydrolysis using LiOH.H₂O in ethanol/water (1:1)³³.

Compound **6** served as a crucial starting point for the synthesis of series 1, 3 and 5 (scheme 2). the titled compounds, **series 1**, (**7a-i**) were prepared by direct coupling of equimolar amounts of the carboxylic acid (**6**) and the respective substituted piperazine in presence of EDC.HCl as coupling agent/ DMAP as a base in dry DMF under N₂ atmosphere³⁴. **Series 3**, compounds (**8a-f**), was prepared though a similar pattern as compounds **7a-i**, by the direct coupling of equimolar amounts of the carboxylic acid (**10**) and the respective amino compounds (**1a-f**, Fig. 3) using EDC.HCl as coupling agent/ DMAP as a base in dry DMF under N₂ atmosphere³⁴. Using the same coupling procedure³⁴, compound (**6**) and the respective amino compounds (**IIa,b**, Fig. 3) were reacted yielding **9a,b**, **series 5**, Fig. 4.

Furthermore, we applied the same above-mentioned coupling procedure to obtain the titled compound (**10**). Compound (**10**) was prepared upon reaction of 3-nitro-4-(phenethylamino)benzoic acid (**3**), which was obtained in good yields (94%) and purity according to Fig. 5, and ethyl 2-amino benzo[*d*]thiazole-6-carboxylate (**4**)³⁴. The titled compound (**10**) was subjected to ester hydrolysis to yield compound (**11**).

According to Fig. 6, compound **11** is considered very important starting building block for the synthesis of **series 2**, **4** and **6**. Compound lists **12a-e**, **13a-d** and **14a,b** were obtained using the same coupling procedure using compound **11** and respective substituted piperazines, amino compounds (**1a-f**) and (**IIa,b**) respectively.

Finally, Fig. 7 illustrates the synthesis of the final compounds **17a-j**, **series 7**. Compound **15** was synthesized according to the reported method where it was produced in good yield and purity³⁵. Furthermore, nitro group in compound **15** was reduced following the reported procedure³⁵. Compound **16** served as crucial starting material to obtain compounds **17a-j**, where it reacted with the respective isocyanate in THF³⁶. The urea derivatives **17a-j**

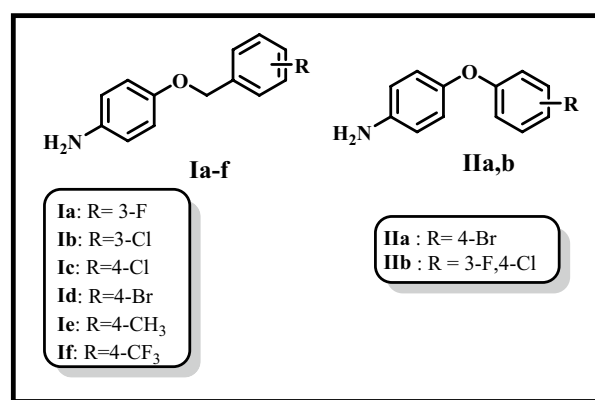


Figure 3. Structures of reported intermediates **Ia-f** and **IIa,b** used in the synthesis of the final compounds.

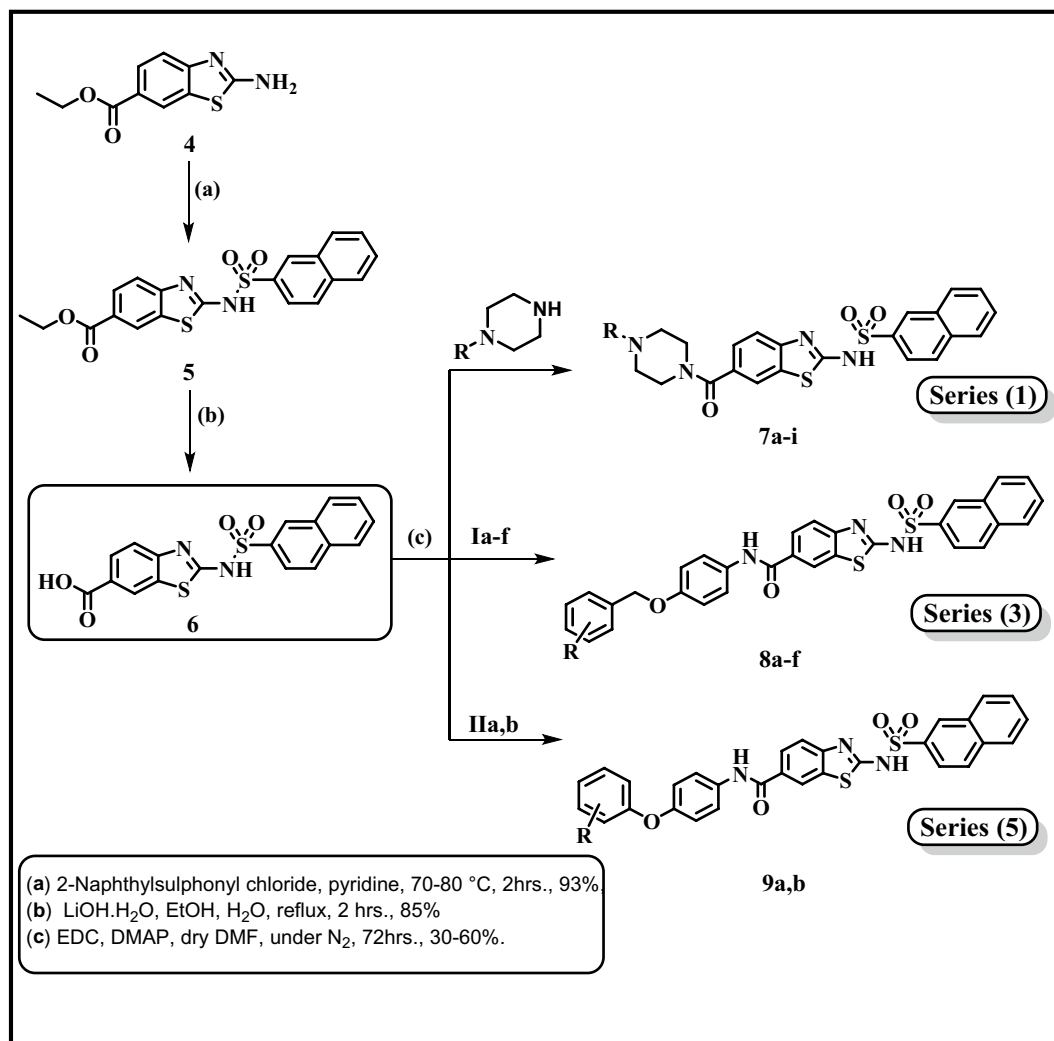


Figure 4. Synthesis of final compounds **7a-i** (Series 1), **8a-f** (Series 3) and **9a,b** (Series 5) **7a:** R = Phenyl, **7b:** R = 2-Fluorophenyl, **7c:** R = 2-Methoxyphenyl, **7d:** R = 3,4 Dichlorophenyl, **7e:** R = 4-Chlorophenyl, **7f:** R = Benzhydryl, **7g:** R = Trans-Cinammyl, **7h:** R = 1-Piperonyl, **7i:** R = 2-Tetrahydrofuroyl, **8a:** R = 3-F, **8b:** R = 3-Cl, **8c:** R = 4-Cl, **8d:** R = 4-Br, **8e:** R = 4-CH₃, **8f:** R = 4-CF₃, **9a:** R = 3-F,4-Cl, **9b:** R = 4-Br.

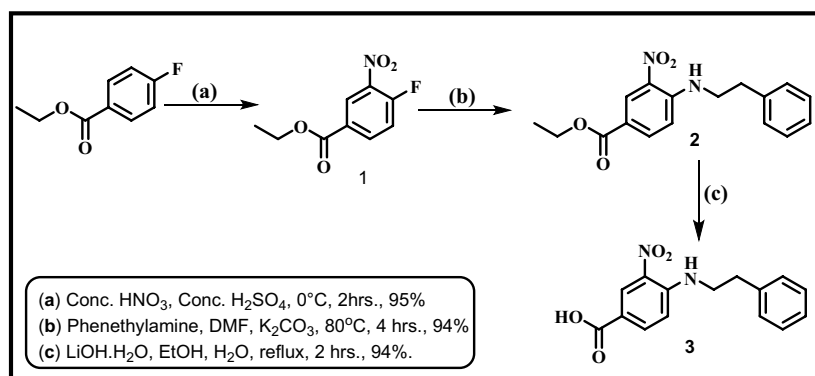


Figure 5. Synthesis of 3-Nitro-4-(phenethylamino) benzoic acid (**3**).

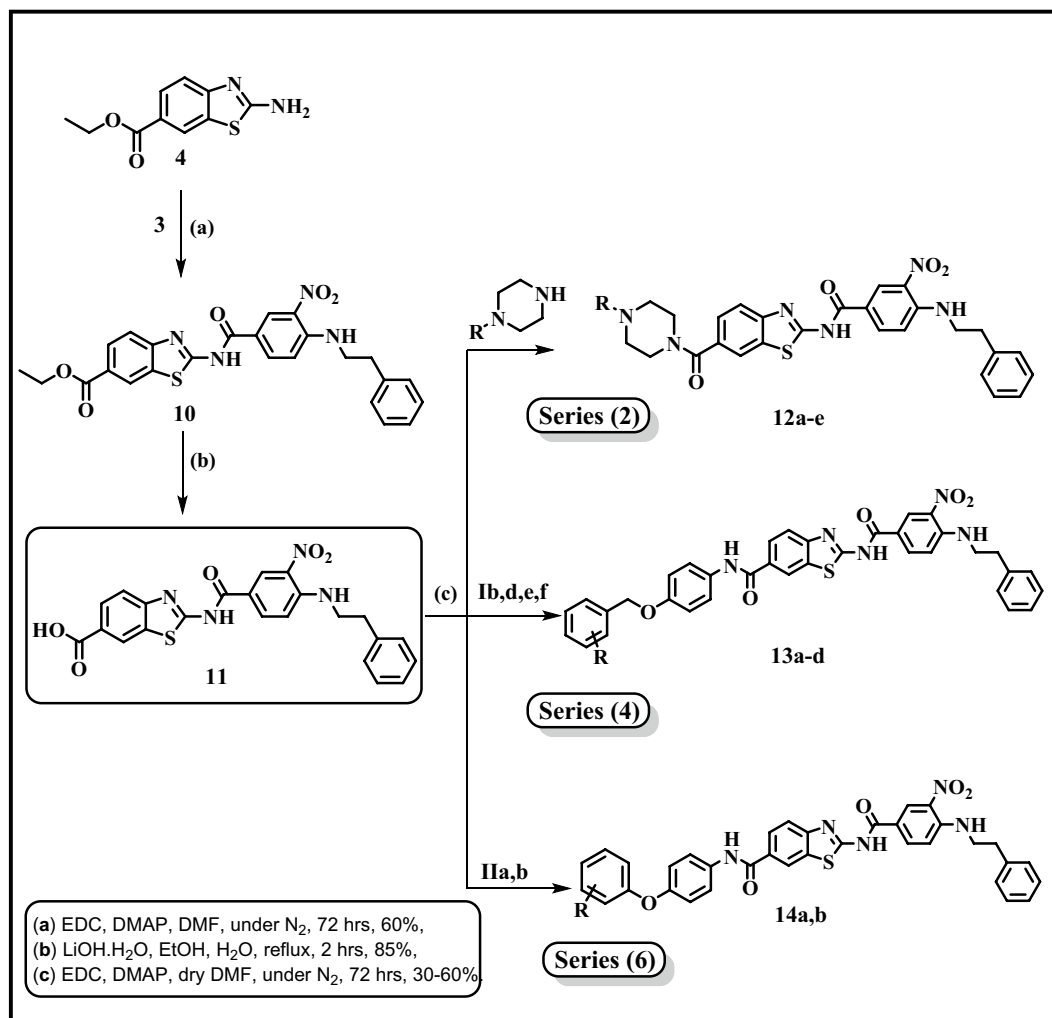


Figure 6. Synthesis of final compounds: **12a-e** (Series 2), **13a-d** (Series 4) and **14a,b** (Series 6); **12a**: R = 2-Methoxyphenyl, **12b**: R = 3,4-Dichlorophenyl, **12c**: R = Benzhydryl, **12d**: R = Trans-Cinammyl, **12e**: R = 2-Tetrahydrofuroyl; **13a**: R = 3-Cl, **13b**: R = 4-Br, **13c**: R = 4-CH₃, **13d**: R = 4-CF₃; **14a**: R = 3-F,4-Cl, **14b**: R = 4-Br.

were obtained in good yield and purity. The structures of all the newly synthesized compounds were confirmed by their spectral data.

Biological evaluation. *Initial in vitro BCL-2 inhibitory screening at single dose of 10 μM concentration.* Our novel synthesized compounds were screened for their potential BCL-2 anti-apoptotic effects. The in vitro BCL-2 inhibition assay was executed at the BPS Bioscience Corporation, San Diego, CA, USA. Table 1 and Fig. 8 illustrate the inhibitory effects of the compounds against BCL-2 protein, which happened to be either very poor or good inhibitory activity.

Regarding the P4 hydrophobic binding moiety, where incorporation of 3-nitro-4-(phenethylamino)benzamide moiety at position 2 of benzothiazole scaffold generally resulted in marked improvement of BCL-2 inhibitory activity when compared to their naphthyl sulfonamide analogues (Series 2, 4 & 6 compared to series 1, 3 & 5). Regarding the P2 hydrophobic binding moiety, para substituted benzyloxyphenyl derivatives (series 3 & 4), compounds (**8c,d** and **13b-d**), exhibited better BCL-2 inhibitory activity than the corresponding phenoxyphenyl derivatives (**13** and **14**). These compounds showed good inhibitory activity with BCL-2 percent inhibition of 48, 65, 68, 84 and 84%, respectively. Moreover, the 3-fluorobenzyloxy derivative (**8a**) and 3-chlorobenzyloxy derivative (**13a**) also exhibited moderate inhibitory activity with BCL-2 percent inhibition of 41 and 35%, respectively. As mentioned above, compounds bearing 3-nitro-4-phenylaminobenzamide tail were superior to their naphthyl sulfonamide analogues (compounds (**13a-d**) versus compounds (**8c-f**)). Regarding the phenoxyphenyl derivatives (series 5 & 6), only the 4-bromo phenoxyphenyl derivative (**14b**) showed moderate BCL-2 inhibitory activity with 47% inhibition. Investigating the urea derived compounds (series 7), also revealed that the 4-bromo phenyl urea derivative (**17f**) exhibited good BCL-2 inhibitory activity with 64% inhibition. On the contrary, the piperazine

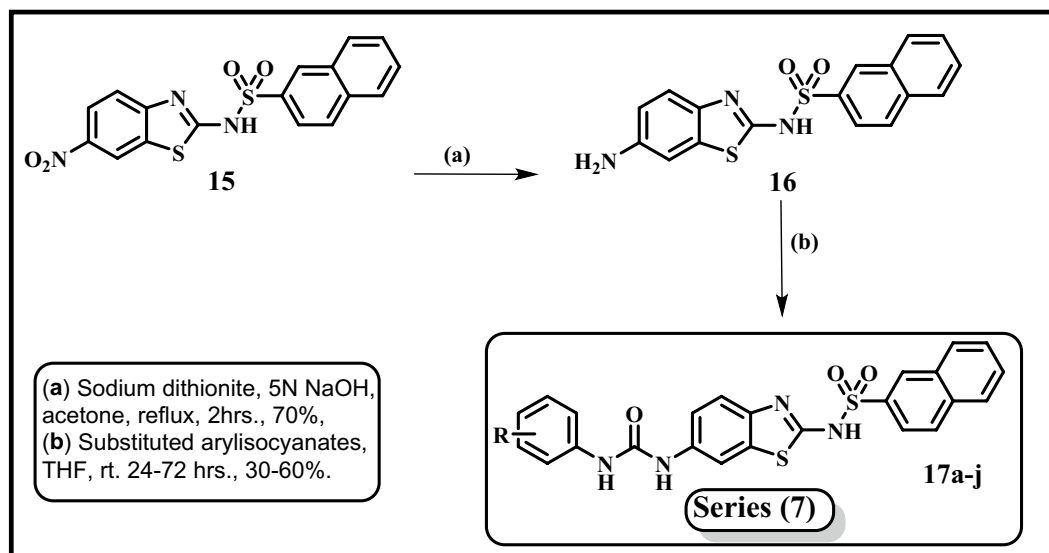


Figure 7. Synthesis of final compounds **17a-j** (Series 7); **17a**: R=H, **17b**: R=3- Cl, **17c**: R=3- Br, **17d**: R=3- O-CH₃, **17e**: R=3-CH₃, **17f**: R=4- Br, **17g**: R=4- Cl, 3-CF₃, **17h**: R=3,4- di Cl, **17i**: R=2-CH₃,4-Cl, **17j**: R=3-Cl,4-CH₃.

ID	BCL-2 inhibition %	ID	BCL-2 inhibition %
7a	0	12c	18
7b	0	12d	14
7c	2	12e	8
7d	8	13a	35
7e	0	13b	68
7f	7	13c	84
7g	7	13d	84
7h	1	14a	20
7i	4	14b	47
8a	41	17a	0
8b	16	17b	7
8c	48	17c	10
8d	65	17d	7
8e	13	17e	0
8f	14	17f	64
9a	9	17g	18
9b	9	17h	0
12a	15	17i	14
12b	18	17j	9
ABT-199 (20)	92 (at 100 nM)		

Table 1. Percent inhibition of BCL-2 inhibitory activity achieved by the piperazine derivatives, **7a-i** (Series 1), **12a-e** (Series 2), benzyloxy derivatives series 3 (**8a-f**), series 4 (**13a-d**), **13a,b** (Series 5), **14a,b** (Series 6), and **17a-j** (Series 7) at 10 μ M.

derivatives (series 1 & 2) showed no or poor inhibitory activity on BCL-2 with 18% as the most achieved inhibition by compounds (**12b** and **12c**), Fig. 9.

Measurement of potential enzyme inhibitory activity (IC₅₀). Promising candidates, which exhibited BCL-2 inhibition percent above 60% at 10 μ M concentration (**8d**, **13b-d** & **17f**) were further investigated for their dose-related BCL-2 inhibitory activity at 5 different concentrations (1 nM–10 nM–100 nM–1 μ M–10 μ M) to subsequently calculate their IC₅₀ values, Table 2.

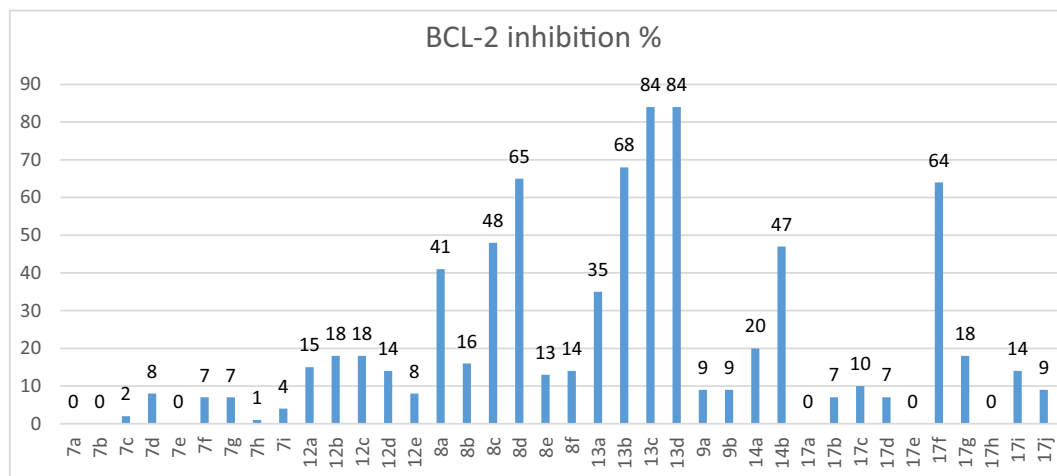


Figure 8. Percent inhibition of BCL-2 inhibitory activity achieved by the newly synthesized compounds.

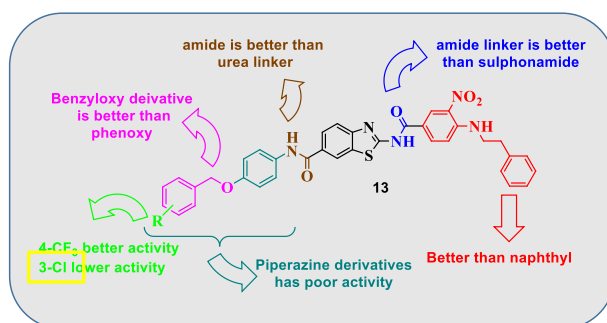


Figure 9. Structure activity relationship diagram showing the most potent compound 13.

ID	BCL-2% inhibition	BCL-2 IC ₅₀
8d	65	1.620 μM
13b	68	1.087 μM
13c	84	0.471 μM
13d	84	0.363 μM
17f	64	2.290 μM
ABT-199 (20)	92 (at 100 nM)	0.007 μM

Table 2. The IC₅₀ values for compounds 8d, 13b-d and 17f. Significant values are in bold.

In vitro anti-proliferative activity against leukemia NCI cell lines. This assay was performed for compounds 13c and 13d by the Developmental Therapeutics Program (DTP) of the National Cancer Institute (NCI), division of cancer treatment and diagnosis, NIH, Bethesda, Maryland, USA (www.dtp.nci.nih.gov). The operation of this screen utilizes leukemia human tumor cell line³⁷. The human tumor cell lines of the cancer screening panel were grown in RPMI 1640 medium containing 5% fetal bovine serum and 2 mM L-glutamine.

Results for the two compounds were reported as a mean graph of the percent growth of the treated cells when compared to the untreated control cells. The results are expressed as cell growth percent for the tested compounds on each of the used NCI cell line panels. Table 3 shows the results for the compounds 13c and 13d.

Compound 13d, which demonstrated the highest inhibitory activity against BCL-2 with IC₅₀ value of **0.363 μM**, exhibited moderate inhibition against leukemic SR cell lines with growth inhibition **62.87**. While compound 13c exhibited poor inhibition against the used leukemia cell line.

Molecular modelling study. The validity of the proposed design was evaluated by molecular docking study through predicting the binding modes and binding affinities of the designed compounds. These predicted properties should meet the minimum desirable requirements to validate the hypothesis that the designed

Cell growth percent for the tested compounds		
Leukemia		
Panel/cell line	13c	13d
CCRF-CEM	93.91	68.2
HL-60(TB)	75.74	96.87
K-562	87.23	67.92
MOLT-4	94.74	74.37
RPMI-8226	87.5	69.86
SR	82.5	37.13

Table 3. Cell growth percentage of NCI leukemia cancer cell line exhibited by the final compounds **13c** and **13d**. Significant values are in bold.

compounds have proposed biological activities against BCL-2. The docking study was performed in order to test for a comparable binding mode to the saccharine lead compound **2** and investigate the binding affinities of the designed compounds to BCL-2 binding groove. The major goal of a good docking protocol is to discriminate between the groups of true solutions (proposed poses), usually defined as poses within 2.0 Å root mean square deviations (RMSD) from the X-ray geometry, and false solutions or misdocked structures³⁸. In order to validate the C-DOCKER protocol's predictability of the correct poses, we re-docked the co-crystallized ligand using C-DOCKER, and aligned the pose retrieved from docking to the X-ray geometry (The co-crystallized bioactive conformation) to calculate the RMSD. The docking of this compound in BCL-2 binding groove generated RMSD of 0.6656 Å (Fig. 10), therefore, the C-DOCKER protocol is reliable for predicting the poses of the tested compounds in the X-ray crystal structure of BCL-2 protein.

The docking study of the synthesized compounds into BCL-2 binding groove revealed comparable binding modes of the docked molecules to the lead compound. Docking of the target compounds showed that the core scaffold adopted volumes and orientation as the lead compound. The docking results showed the designed compounds to have C-Docker interaction energies ranging from – 67.57 to – 40.31 kcal/mole which came comparable to the docking score of the co-crystallized ligand with docking score of – 71.89 kcal/mol. The docking score of the 5 most active compounds come in a good agreement with their IC₅₀, where they are ranked in the same order according to the IC₅₀ order. They are arranged from the most active to the least active as follows: 13d > 13c > 13b > 8d > 17f, as shown in Table 4.

P-substituted-benzyloxyphenyl derivatives (**series 3 & 4**), exhibited the best BCL-2 inhibitory activity as they fulfilled most of the key interactions with BCL-2, where the key hydrogen bonds with Gly 104 and Arg 66 residues were established (as seen in compounds **13c** & **13d**, which are the most active compounds against BCL-2), as well as a pi–pi interaction with Tyr67 and Tyr161. Also, pi-alky interactions were observed with various amino acid residues (Arg 98, Ala 59 & Pro163) resulting in better docking scores as well, which could explain the good BCL-2 inhibitory activity of those compounds (Fig. 11A and B).

Regarding the moderately active compounds (**8a,c,d**, **13b**, **14b** & **17f**), they showed the same binding mode and interactions as the most active compounds (**13c** & **13d**) but they missed a key HB with Gly 104 which could explain its moderate activity (Fig. 12). However, they formed another H-bond with Arg 105 residue compensating the loss of the main HB with Gly 104 (Table S1).

On the contrary, piperazine derivatives (**series 1 & 2**) failed to exhibit BCL-2 inhibitory activity as they missed the key interaction with Gly104 residue which seemed to be an essential feature for BCL-2 inhibitory activity, although they maintained the same binding mode and the same key hydrogen bond with Arg 66 and hydrophobic interactions (Pi-Pi) with Tyr 67, Tyr 161. Generally, most of inactive compounds missed this key hydrogen bond interaction with Gly 104 residue. Moreover, they showed lower docking scores relative to that of the docked lead

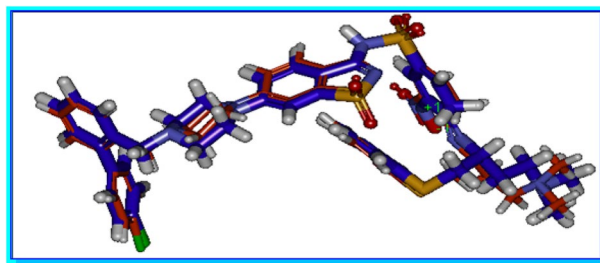
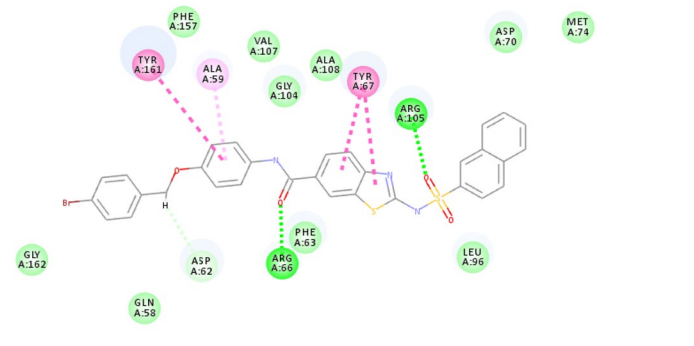
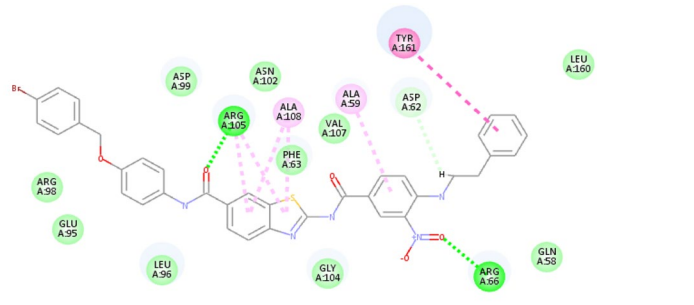
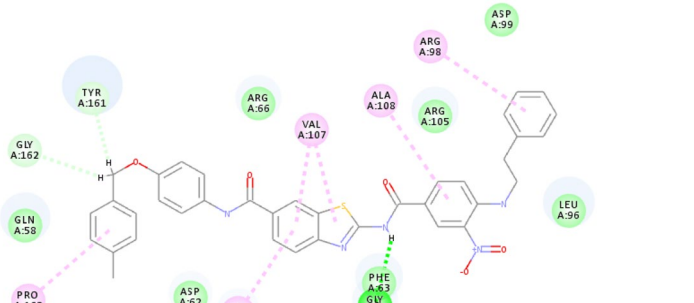


Figure 10. The alignment between the co-crystallized bioactive conformer of compound (**blue**) and the pose of the same compound retrieved from docking using CDOCKER (**orange**). Figure 10 was generated using Discovery studio 2.5.

ID	2D interaction diagram	C-docker interaction energy & binding interactions		
8d	 <p>Interactions</p> <ul style="list-style-type: none"> ■ van der Waals ■ Conventional Hydrogen Bond ■ Carbon Hydrogen Bond ■ Pi-Pi T-shaped ■ Pi-Alkyl 	<p>-53.08</p> <p>HBA Arg 66</p> <p>HBA Arg 105</p> <p>Pi-Pi Tyr 67</p> <p>Pi-Pi Tyr 161</p>		
	13b	 <p>Interactions</p> <ul style="list-style-type: none"> ■ van der Waals ■ Conventional Hydrogen Bond ■ Carbon Hydrogen Bond ■ Pi-Pi T-shaped ■ Pi-Alkyl 	<p>-55.83</p> <p>HBA Arg 66</p> <p>HBA Arg 105</p> <p>Pi-Pi Tyr 161</p>	
		13c	 <p>Interactions</p> <ul style="list-style-type: none"> ■ van der Waals ■ Conventional Hydrogen Bond ■ Carbon Hydrogen Bond ■ Pi-Alkyl 	<p>-58.05</p> <p>HBA Gly 104</p> <p>Pi-Alkyl Ala 59</p> <p>Pi-Alkyl Arg 98</p> <p>Pi-Alkyl Val 107</p> <p>Pi-Alkyl Ala 108</p> <p>Pi-Alkyl Pro 163</p>
			Continued	

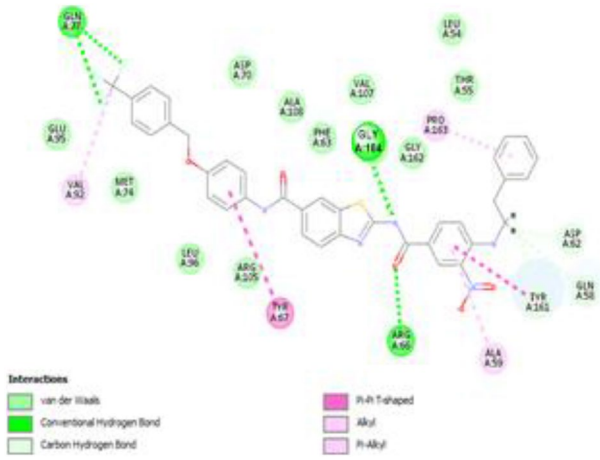
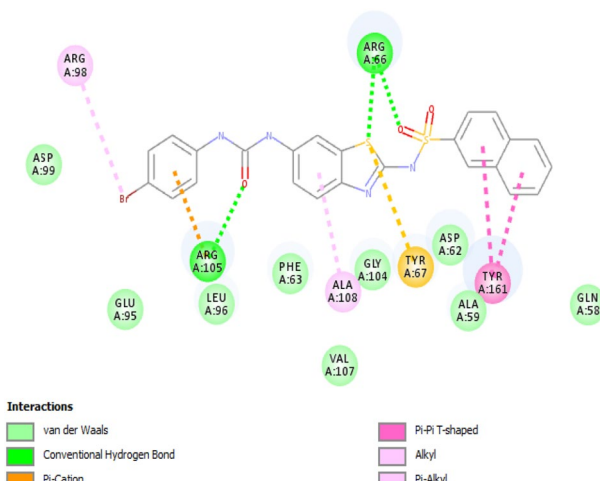
ID	2D interaction diagram	C-docker interaction energy & binding interactions
13d		-59.15
		HBA Gly 104
		Pi-Pi Tyr 67
		Pi-Pi Tyr 161
		Pi- Pi-Alkyl Ala 59
		Pi-Alkyl Val 92
Pi-Alkyl Pro 163		
17f.		-41.69
		HBA Arg 66
		HBA Arg 105
		Pi-Pi Tyr 161
		Pi- Sulfur Tyr 67
		Pi- Alkyl Arg 98
Pi- Alkyl Ala 108		

Table 4. Docking scores, 2D interaction diagrams, and interacting amino acids with compounds **8d**, **13b-d** and **17f**.

compound. 2D interactions, docking scores, and detailed binding interactions for active compounds with BCL-2 inhibition > 50% are reported in Table S1 in supporting info.

Physicochemical and drug likeness properties. The *in silico* physicochemical properties of the reported compounds were calculated using SwissADME web server. Six parameters that detect the oral bioavailability were calculated namely number of rotatable bonds, Solubility Log S, fraction of sp³ carbons, Topological polar surface area (TPSA), molecular weight (MW), and XLOGP3 for lipophilicity, as shown in Fig. 13. Most of the compounds showed acceptable number of rotatable bonds (<9), TPSA (<130 Å²), and sp³ carbon fraction (<1). Most of the compounds showed moderate water solubility (ESOL Log S < -6), slightly high molecular weight (>500), and high lipophilicity (XLOGP3 > 5). These results gave a basis for further drug development for the reported series to adjust the lipophilic/hydrophilic balance, solubility, and molecular weight.

The drug likeness for the reported compounds was also predicted using SwissADME web server by calculating five filters namely, Lipinski, Ghose, Veber, Egan, and Muegge. The results were reported by the number of violations each compound commits per filter in Table 5. The results are depicted as a heat map. Most compounds fulfil all the filters except for the Ghose filter which come from higher molecular weight and molar refractivity. This also can be exploited in prospective drug development projects by adjusting the molecular weight of the designed compounds.

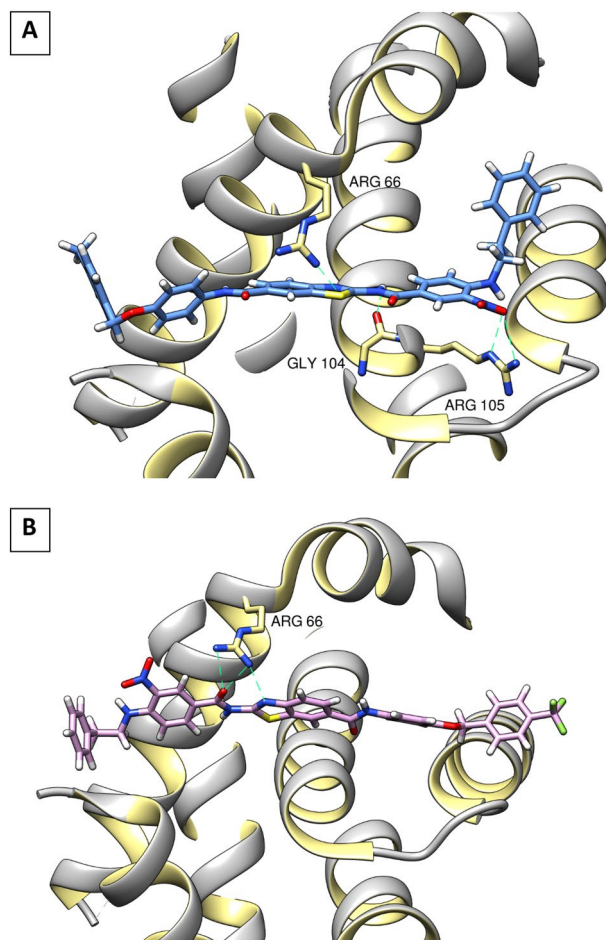


Figure 11. 3D interaction diagram of the most active compounds **13c** (A) and **13d** (B) with BCL-2 BH3 binding groove. Figure 11 was generated using Chimera 1.16 (<https://www.cgl.ucsf.edu/chimera/>).

Conclusion

Our main approach was to design new small molecules as BCL-2 inhibitors with potential anti-cancer activity based on literature review and SAR studies, novel benzothiazole-based compounds were designed, synthesized and evaluated for their in vitro BCL-2 inhibitory activity. The 4-CH₃ and 4-CF₃ benzyloxy derivatives (**13c** & **13d**) having 3-nitro-4-phenethyl amino moiety as the P4 hydrophobic binding group, exhibited the highest inhibitory activity against BCL-2 protein with IC₅₀ values of 0.471 and 0.363 μM, respectively. The designed and synthesized compounds could act as a potential cornerstone for future design of more potent and selective BCL-2 inhibitors and hence promising anticancer agents.

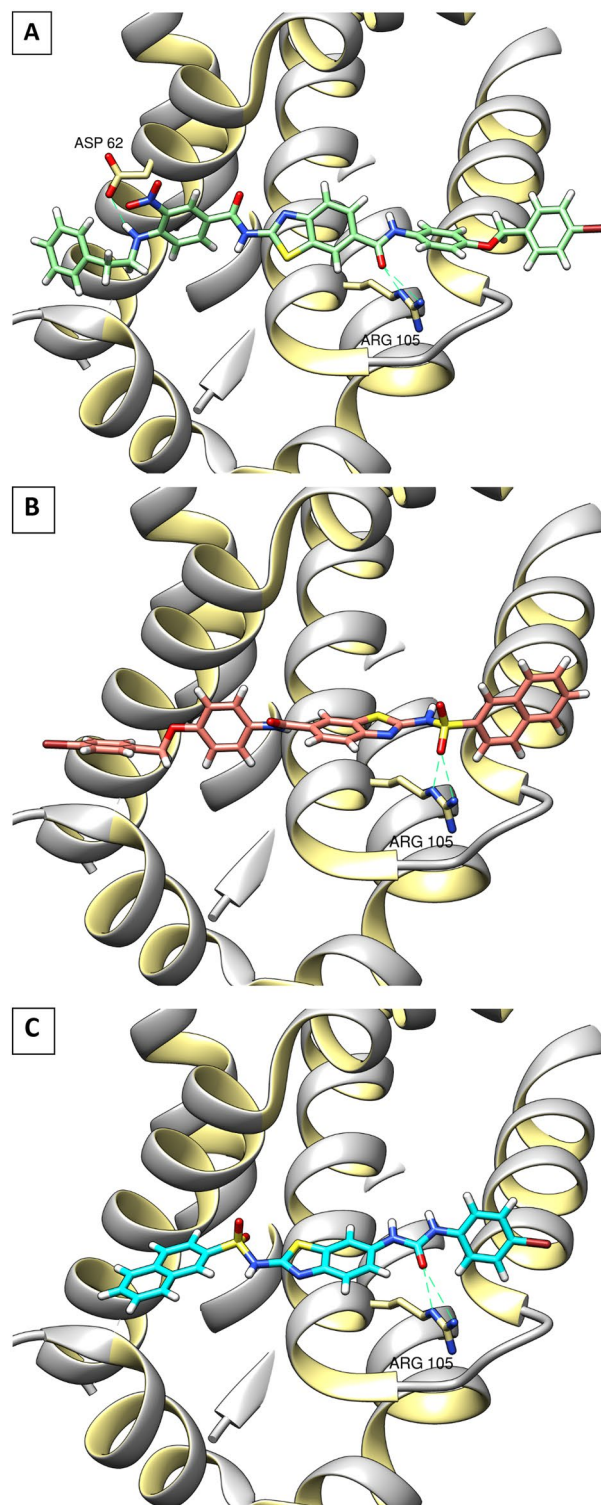


Figure 12. 3D interaction diagram of the compounds **13b** (A), **8d** (B) & **17f** (C) with BCL-2 BH3 binding groove. Figure 12 was generated using Chimera 1.16 (<https://www.cgl.ucsf.edu/chimera/>).

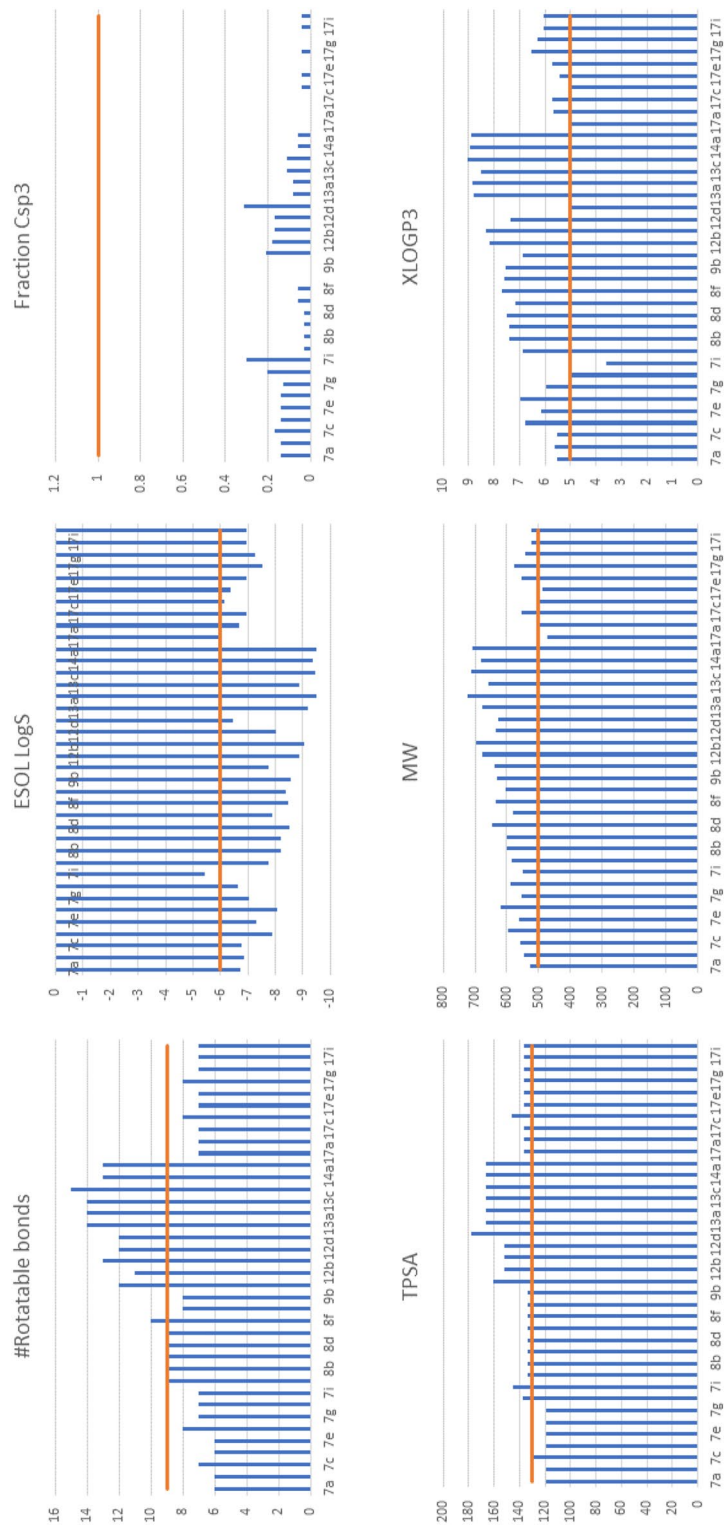


Figure 13. Six physicochemical properties that determine the bioavailability, number of rotatable bonds, solubility ESOL LogS, sp3 carbon fraction, topological polar surface area (TPSA), molecular weight (MW), lipophilicity (XLOGP3). That upper/lower cutoff for each property is drawn in orange horizontal line.

ID	Lipinski	Ghose	Veber	Egan	Muegge
7a	1	2	0	0	1
7b	1	3	0	1	1
7c	1	2	0	0	1
7d	2	3	0	1	1
7e	1	3	0	1	1
7f	2	4	0	1	2
7g	1	3	0	0	1
7h	1	2	0	1	1
7i	1	2	1	1	0
8a	2	3	0	2	1
8b	2	3	0	2	2
8c	2	3	0	2	2
8d	2	3	0	2	2
8e	2	3	0	2	1
8f	2	3	0	2	2
9a	2	3	0	2	2
9b	2	3	0	2	2
12a	2	3	2	1	3
12b	1	4	2	2	3
12c	1	4	2	2	3
12d	1	3	2	1	3
12e	2	3	2	1	2
13a	2	4	2	2	3
13b	2	4	2	2	3
13c	1	4	2	2	3
13d	2	4	2	2	3
14a	2	4	2	2	3
14b	2	4	2	2	3
17a	0	2	0	2	1
17b	1	3	0	2	1
17c	1	3	0	2	1
17d	1	3	1	2	1
17e	0	3	0	2	1
17f	1	3	0	2	1
17g	2	3	0	2	1
17h	2	3	0	2	1
17i	1	3	0	2	1
17j	1	3	0	2	1

Table 5. The predicted Drug likeness for the synthesized compounds using SwissADME web server.

Data availability

All data generated or analysed for this study are included in this published paper (and its Supplementary Information files).

Received: 9 March 2023; Accepted: 31 August 2023

Published online: 20 September 2023

References

1. Avendaño, C. & Menéndez, J. C. *Medicinal Chemistry of Anticancer Drugs* 2nd edn, 1–740 (Elsevier, 2015).
2. Hanahan, D. & Weinberg, R. A. Hallmarks of cancer: The next generation. *Cell* **144**(5), 646–674 (2011).
3. Renehan, A. G., Booth, C. & Potten, C. S. What is apoptosis, and why is it important?. *BMJ* **322**(7301), 1536–1538 (2001).
4. Soliman, A. M. *et al.* Induction of apoptosis, cytotoxicity and radiosensitization by novel 3,4-dihydroquinazolinone derivatives. *Bioorg. Med. Chem. Lett.* **49**, 128308 (2021).
5. Wong, R. S. Y. Apoptosis in cancer: From pathogenesis to treatment. *J. Exp. Clin. Cancer Res.* **30**(1), 87 (2011).
6. Kasibhatla, S. & Tseng, B. Why target apoptosis in cancer treatment?. *Mol. Cancer Ther.* **2**(6), 573–580 (2003).
7. Boice, A. & Bouchier-Hayes, L. Targeting apoptotic caspases in cancer. *Biochim. Biophys. Acta Mol. Cell Res.* **1867**(6), 118688 (2020).
8. Van Opdenbosch, N. & Lamkanfi, M. Caspases in cell death, inflammation, and disease. *Immunity* **50**(6), 1352–1364 (2019).

9. Garrido, C. *et al.* Mechanisms of cytochrome c release from mitochondria. *Cell Death Differ.* **13**(9), 1423–1433 (2006).
10. Pfeffer, C. M. & Singh, A. T. K. Apoptosis: A target for anticancer therapy. *Int. J. Mol. Sci.* **19**, E448. <https://doi.org/10.3390/ijms19020448> (2018).
11. Reed, J. C. & Pellecchia, M. Apoptosis-based therapies for hematologic malignancies. *Blood* **106**(2), 408–418 (2005).
12. Adams, J. M. & Cory, S. The Bcl-2 apoptotic switch in cancer development and therapy. *Oncogene* **26**(9), 1324–1337 (2007).
13. Kale, J., Osterlund, E. J. & Andrews, D. W. BCL-2 family proteins: Changing partners in the dance towards death. *Cell Death Differ.* **25**(1), 65–80 (2018).
14. Warren, C. F. A., Wong-Brown, M. W. & Bowden, N. A. BCL-2 family isoforms in apoptosis and cancer. *Cell Death Dis.* **10**(3), 177 (2019).
15. Kroemer, G., Galluzzi, L. & Brenner, C. Mitochondrial membrane permeabilization in cell death. *Physiol. Rev.* **87**(1), 99–163 (2007).
16. Hata, A. N., Engelman, J. A. & Faber, A. C. The BCL2 family: Key mediators of the apoptotic response to targeted anticancer therapeutics. *Cancer Discov.* **5**(5), 475–487 (2015).
17. Kvasnakul, M. & Hinds, M. G. The Bcl-2 family: Structures, interactions and targets for drug discovery. *Apoptosis* **20**(2), 136–150 (2015).
18. Chan, S. L. & Yu, V. C. Proteins of the bcl-2 family in apoptosis signalling: From mechanistic insights to therapeutic opportunities. *Clin. Exp. Pharmacol. Physiol.* **31**(3), 119–128 (2004).
19. Youle, R. J. & Strasser, A. The BCL-2 protein family: Opposing activities that mediate cell death. *Nat. Rev. Mol. Cell Biol.* **9**(1), 47–59 (2008).
20. Obeng, E. Apoptosis (programmed cell death) and its signals—A review. *Braz J Biol* **81**(4), 1133–1143 (2021).
21. Shimizu, S. *et al.* Role of Bcl-2 family proteins in a non-apoptotic programmed cell death dependent on autophagy genes. *Nat. Cell Biol.* **6**(12), 1221–1228 (2004).
22. Reed, J. S. *et al.* The role of MHC class I allele Mamu-A*07 during SIV(mac)239 infection. *Immunogenetics* **63**(12), 789–807 (2011).
23. Khan, K. H., Blanco-Codesido, M. & Molife, L. R. Cancer therapeutics: Targeting the apoptotic pathway. *Crit. Rev. Oncol. Hematol.* **90**(3), 200–219 (2014).
24. Kapoor, I. *et al.* Targeting BCL-2 in B-cell malignancies and overcoming therapeutic resistance. *Cell Death Dis.* **11**(11), 941 (2020).
25. Ishikawa, M. & Hashimoto, Y. Improvement in aqueous solubility in small molecule drug discovery programs by disruption of molecular planarity and symmetry. *J. Med. Chem.* **54**(6), 1539–1554 (2011).
26. Sleebs, B. E. *et al.* Quinazoline sulfonamides as dual binders of the proteins B-cell lymphoma 2 and B-cell lymphoma extra long with potent proapoptotic cell-based activity. *J. Med. Chem.* **54**(6), 1914–1926 (2011).
27. Perez, H. L. *et al.* Identification of a phenylacetylsulfonamide series of dual Bcl-2/Bcl-xL antagonists. *Bioorg. Med. Chem. Lett.* **22**(12), 3946–3950 (2012).
28. Schroeder, G. M. *et al.* Pyrazole and pyrimidine phenylacetylsulfonamides as dual Bcl-2/Bcl-xL antagonists. *Bioorg. Med. Chem. Lett.* **22**(12), 3951–3956 (2012).
29. Touré, B. B. *et al.* The role of the acidity of N-heteroaryl sulfonamides as inhibitors of bcl-2 family protein-protein interactions. *ACS Med. Chem. Lett.* **4**(2), 186–190 (2013).
30. Filippakopoulos, P. *et al.* Histone recognition and large-scale structural analysis of the human bromodomain family. *Cell* **149**(1), 214–231 (2012).
31. Berman, H. M. *et al.* The protein data bank. *Nucleic Acids Res.* **28**(1), 235–242 (2000).
32. Pettersen, E. F. *et al.* UCSF Chimera—a visualization system for exploratory research and analysis. *J. Comput. Chem.* **25**(13), 1605–1612 (2004).
33. Gibson, C. L. *et al.* Diversity oriented syntheses of fused pyrimidines designed as potential antifolates. *Org. Biomol. Chem.* **7**(9), 1829–1842 (2009).
34. Leow, M. L. *et al.* Benzofuran-based estrogen receptor α modulators as anti-cancer therapeutics: In silico and experimental studies. *Curr. Med. Chem.* **20**(22), 2820–2837 (2013).
35. González-Alvarez, M. *et al.* Development of novel copper(II) complexes of benzothiazole- N-sulfonamides as protective agents against superoxide anion. Crystal structures of [Cu(N-2-(4-methylbenzothiazole)benzenesulfonamidate)(2)(py)(2)] and [Cu(N-2-(6-nitrobenzothiazole)naphthalenesulfonamidate)(2)(py)(2)]. *J. Biol. Inorg. Chem.* **8**(12), 112–20 (2003).
36. Manoharan, D. *et al.* Synthesis, characterization and evaluation of antidiabetic activity of novel indoline derivatives. *Bangladesh J. Pharmacol.* **12**, 20 (2017).
37. Shoemaker, R. H. The NCI60 human tumour cell line anticancer drug screen. *Nat. Rev. Cancer* **6**(10), 813–823 (2006).
38. Wu, G. *et al.* Detailed analysis of grid-based molecular docking: A case study of CDOCKER-A CHARMM-based MD docking algorithm. *J. Comput. Chem.* **24**(13), 1549–1562 (2003).

Author contributions

H.S.I.: Participated to the design, conducting chemical experiment and writing the manuscript; A.K.: Participated in conducting chemical experiments, performed the molecular docking and participated to the writing of the manuscript; R.A.T.: Conducted the biological experiments, data analysis and writing the biology part of the manuscript; D.S.L.: Designed the chemistry experiments, analyzed and interpreted the data; D.A.A.E.: Participated to the design and rational, supervision of the chemical experiments and overall writing of the manuscript.

Funding

Open access funding provided by The Science, Technology & Innovation Funding Authority (STDF) in cooperation with The Egyptian Knowledge Bank (EKB).

Competing interests

The authors declare no competing interests.

Additional information

Supplementary Information The online version contains supplementary material available at <https://doi.org/10.1038/s41598-023-41783-1>.

Correspondence and requests for materials should be addressed to A.K. or D.A.A.E.

Reprints and permissions information is available at www.nature.com/reprints.

Publisher's note Springer Nature remains neutral with regard to jurisdictional claims in published maps and institutional affiliations.



Open Access This article is licensed under a Creative Commons Attribution 4.0 International License, which permits use, sharing, adaptation, distribution and reproduction in any medium or format, as long as you give appropriate credit to the original author(s) and the source, provide a link to the Creative Commons licence, and indicate if changes were made. The images or other third party material in this article are included in the article's Creative Commons licence, unless indicated otherwise in a credit line to the material. If material is not included in the article's Creative Commons licence and your intended use is not permitted by statutory regulation or exceeds the permitted use, you will need to obtain permission directly from the copyright holder. To view a copy of this licence, visit <http://creativecommons.org/licenses/by/4.0/>.

© The Author(s) 2023